Protein Expression and Purification 138 (2017) 69–75

Contents lists available at ScienceDirect

Protein Expression and Purification

journal homepage: www.elsevier.com/locate/yprep

Functional characterization of a soluble NADPH-cytochrome P450 reductase from *Fusarium graminearum*

Thomas Etzerodt [a, *], Karl Wetterhorn [b], Giuseppe Dionisio [c], Ivan Rayment [b]

[a] Department of Agroecology, Aarhus University, Forsøgsvej 1, 4200 Slagelse, Denmark
[b] Department of Biochemistry, University of Wisconsin, Madison, WI 53706, United States
[c] Department of Molecular Biology and Genetics, Aarhus University, Forsøgsvej 1, 4200 Slagelse, Denmark

ARTICLE INFO

Article history:
Received 23 April 2017
Received in revised form
24 June 2017
Accepted 3 July 2017
Available online 6 July 2017

Keywords:
Cytochrome *c*
Thiazolyl blue tetrazolium bromide
Enzyme kinetics
Trichothecenes
Sterol biosynthesis

ABSTRACT

Fusarium head blight is a devastating disease in wheat caused by some fungal pathogens of the *Fusarium* genus mainly *F. graminearum*, due to accumulation of toxic trichothecenes. Most of the trichothecene biosynthetic pathway has been mapped, although some proteins of the pathway remain uncharacterized, including an NADPH-cytochrome P450 reductase. We subcloned a *F. graminearum* cytochrome P450 reductase that might be involved in the trichothecene biosynthesis. It was expressed heterologously in *E. coli* as N-terminal truncated form with an octahistidine tag for purification. The construct yielded a soluble apoprotein and its incubation with flavins yielded the corresponding monomeric holoprotein. It was characterized for activity in the pH range 5.5–9.5, using thiazolyl blue tetrazolium bromide (MTT) or cytochrome *c* as substrates. Binding of the small molecule MTT was weaker than for cytochrome *c*, however, the rate of MTT reduction was faster. Contrary to other studies of cytochrome reductase proteins, MTT reduction proceeded in a cooperative manner in our studies. Optimum kinetic activity was found at pH 7.5–8.5 for bothMTT and cytochrome *c*. This is the first paper presenting characterization of a cytochrome P450 reductase from *F. graminearum* which most likely is involved in mycotoxin biosynthesis or some primary metabolic pathway such as sterol biosynthesis in *F. graminearum*.

1. Introduction

Fusarium head blight is a devastating disease in wheat caused by infection fungal pathogens of the *Fusarium* genus, particularly *Fusarium graminearum*. The pathogen causes significant yield losses [1] due to the accumulation of trichothecene mycotoxins in the cereal heads with deoxynivalenol as the dominant trichothecene [2]. In addition, trichothecenes acts as virulence factors promoting spread of the fungal pathogen within the cereal heads [3,4].

The trichothecene biosynthetic pathway has been mapped extensively for *F. sporotrichioides* and *F. graminearum* [5–8]. TRI5 converts farnesyl pyrophosphate to trichodiene [6,9], which in turn is converted to isotrichodermol by TRI4, an NADPH-dependent cytochrome P450 (CYP) [10,11]. Other identified CYPs of the trichothecene biosynthetic pathway are TRI1, TRI11 and TRI13, which perform hydroxylation of C8, C15 and C4 positions on the trichothecene skeleton, respectively [12–14]. Important CYPs characterized from *F. graminearum* not part of the trichothecene biosynthesis are three CYP51 paralogues [15], Fg08079 of the butenolide biosynthesis [16] and CLM2 of the culmorin biosynthesis [17]. All of the above CYPs have been functionally characterized in fungi but have not yet been isolated and characterized *in vitro* so far.

CYPs require an NADPH-cytochrome P450 reductase (CPR) partner for electron transfer from NADPH to the CYP heme core. CPR proteins contain flavins, which mediate such electron transfer in a highly regulated fashion [18,19]. For *F. graminearum* only two CPR genes have been putatively identified (compared to 107 CYP genes) [20]. Consequently, a single CPR must interact with numerous CYPs and therefore be involved in several diverse biosynthetic pathways. In eukaryotes, like *Fusarium* fungi, CYPs and their reductase partners are membrane bound via an N-terminal anchor, which is required for assembly and activity of CPR-CYP pairs in some cases [21], even though some soluble truncated

Abbreviations: CYP, Cytochrome P450; CPR, NADPH-cytochrome P450 reductase; FgCPR, *Fusarium graminearum* NADPH-cytochrome P450 reductase with N-terminal truncation (Δ1-28) and His_8-tag; Cyt *c*, Cytochrome *c*; MTT, thiazolyl blue tetrazolium bromide.

* Corresponding author.
E-mail addresses: thomas.etzerodt@agro.au.dk, thomas@priceless.dk (T. Etzerodt).

http://dx.doi.org/10.1016/j.pep.2017.07.001
1046-5928/

yeast and fungal CPRs retain their ability to reduce their CYP partners [22–24].

Comparison of kinetics for CPRs from different sources can be complicated since CPR-CYP complexes are highly variable and the specific CYP partner for the CPR of interest is not always available. Although not the natural substrate, *in vitro* reduction of Cyt *c* serves as a general electron acceptor to compare the activity of different CPR proteins [22,25,26]. Other commonly used electron acceptors in activity studies of CPRs are ferricyanide [27], 1,1-diphenyl-2-picrylhydrazyl [27], and thiazolyl blue tetrazolium bromide (MTT), the latter having the best stability and highest molar absorptivity [27,28].

The best studied reductase from the *Fusarium* genus is the nitric oxide reductase from *F. oxysporum* [29–31], but so far no NADPH-cytochrome P450 reductases from *Fusarium* have been isolated for characterization. In this paper we present the characterization of a soluble N-terminally truncated CPR from *F. graminearum*.

2. Materials and methods

2.1. Selection of G-blocks for cloning of the His_8-FgCPRΔ1-28 fragment

A CPR gene has been identified for the *F. graminearum* PH-1 strain [32]. Based on the ORF (~2200 bp), two G-block oligos were designed as C-t and N-t part of the CPR (see Table S 1 in suppl. mat.) with an internal overlap of 23 bp for initial PCR merging to get the full length *FgCPRΔ1-28* gene. Each G-block contained flanking sequences for restriction free (RF) cloning into a target vector. G-blocks, primers for cloning and Sanger sequencing were obtained from Integrated DNA Technologies (IDT, Coralville, IA, USA) and sequences are given in Table S 1 (of Suppl. Mat.).

2.2. Cloning and expression of the His_8-FgCPRΔ1-28 construct

All cloning procedures were performed using RF cloning [33,34]. The *FgCPRΔ1-28* gene fragment was purified by gel electrophoresis from a 1% agarose gel stained with SYBR Green I. The *FgCPRΔ1-28* fragment was cloned into a pTEV4 target vector with kanamycin resistance (from Novagen) downstream a His_8-tag (for details see Suppl. Mat.). DH5α cells were transformed with the *FgCPRΔ1-28:pTEV4* construct. LB culture was grown from a single DH5α colony and plasmids were purified using a Spin Miniprep kit (Qiagen). The resulting *FgCPRΔ1-28* ORF was verified by Sanger sequencing.

CODON + cells (Stratagene) were transformed with the *FgCPRΔ1-28:pTEV4* plasmid. Transformed *E. coli* CODON + single colony was used to inoculate an overnight LB pre-culture which was used to inoculate a 10 l main expression LB culture. When OD_{600} reached 0.8–1 the 10 L culture was cooled to 16 °C. Protein expression was then induced with 1 mM IPTG and the culture was incubated at 16 °C for 24 h. Cells were harvested by centrifugation at 3000 *g* (4 °C). The pellet was frozen in liquid nitrogen and stored at −80 °C until lysis and protein purification.

2.3. Purification of apo His_8-FgCPRΔ1-28 and incorporation of flavins

All purification steps were carried out on ice or at 4 °C. Buffer A was 50 mM Tris (pH 7.5), 0.1 mM EDTA, 1 mM TCEP, 10% glycerol. Frozen cells were re-suspended in 40 ml ice-cold buffer A plus 50 mM NaCl and 0.5 mg/ml lysozyme. The cell suspension was then lysed by sonication, clarified by centrifugation (at 80000 g and 4 °C for 30 min) and the NaCl concentration of the supernatant was brought to 300 mM prior to purification on a 6 ml NiNTA column (Qiagen). The unbound proteins (pass through) and the washed proteins (Buffer A with 300 mM NaCl and 20 mM imidazole) possessed only negligible amount of His-tagged proteins as evaluated by SDS-PAGE and western with anti-HIS_5 antibodies (Qiagen, data not shown). The bound proteins were eluted in 30 ml elution buffer (30 mM Tris/HCl pH 7.5, 0.3 M NaCl and 300 mM Imidazole). The purified FgCPR apo protein was incubated with FMN and FAD (TCI Chemicals, Cambridge, MA) overnight at 4 °C in 10 and 5 M excess, respectively, based on the stoichiometry of a *S. cerevisiae* CPR [35]. Unbound flavins were removed by a second NiNTA purification and the protein solution was concentrated by ultrafiltration (Amicon Ultra-15 Centrifugal Filters, MWCO of 30 kDa; Merck Millipore Ltd, Billerica, MA) and then dialyzed against Buffer A without EDTA. Finally, the protein solution was flash frozen in liquid nitrogen (30 µl aliquots) and stored at −80 °C until analysis.

2.4. Protein characterization

2.4.1. Purity, spectral analysis and aggregation state of FgCPR

Protein concentration was determined spectrophotometrically from its absorbance at 280 nm (corrected for FAD and FMN absorbance) and confirmed by Bradford analysis. Flavin incorporation was assessed from spectral analysis (see Fig. 2) identical to CPRs in other studies [24,36]. Protein purity was assessed by SDS-PAGE. Briefly, FgCPR samples were boiled in 2xSDS buffer (0.1 M Tris (pH 8.0), 10 mM EDTA, 0.1 M DTT, 60% glycerol and 0.05% Bromo Phenol Blue) for 10 min, cooled to RT and 15 µl boiled sample was run on a NuPAGE 4–12% Bis-Tris Gel (ThermoFischer Scientific, Roskilde, Denmark).

Protein aggregation state was assessed by size exclusion chromatography (100 µl of 1.33 mg/ml protein) on an Amersham Superdex 200 HR 10/30 column (300 × 10 mm) using a 20 mM Tris, 1 mM TCEP, 10% ethylene glycol eluent (pH 7.5) with a flow rate of 0.5 ml/min. Apparent molecular weight was determined from comparison with protein markers (cytochrome *c*, carbonic anhydrase, bovine serum albumin, alcohol dehydrogenase and β-amylase from Sigma, St. Louis, MO).

2.4.2. Verification of primary sequence by LC-MS based proteomics

50 µg FgCPR was denatured and reduced in 100 mM ammonium bicarbonate buffer, pH 8.0 (ABC) containing 3.84 M guanidinium chloride and 20 mM DTT, followed by alkylation with iodoacetamide (IAM, 23.8 mM). Excess IAM was then quenched with DTT. The samples were desalted by immobilization on Supel-Tips C18 Micropipette tips (Sigma-Aldrich, Brøndby, Denmark) and the

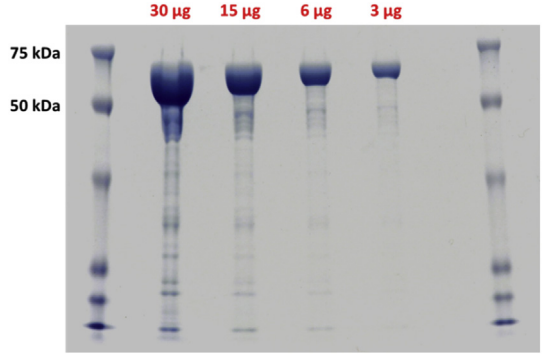

Fig. 1. Analysis of FgCPR by SDS-PAGE and Coomassie R-250 staining of different amounts of protein loaded (as indicated in red). Reference bands are given for protein markers of 50 and 75 kDa from (SDS-prestained Precision Plus Protein Standards, All Blue, BioRad Cat. Num #161–0373). (For interpretation of the references to colour in this figure legend, the reader is referred to the web version of this article.)

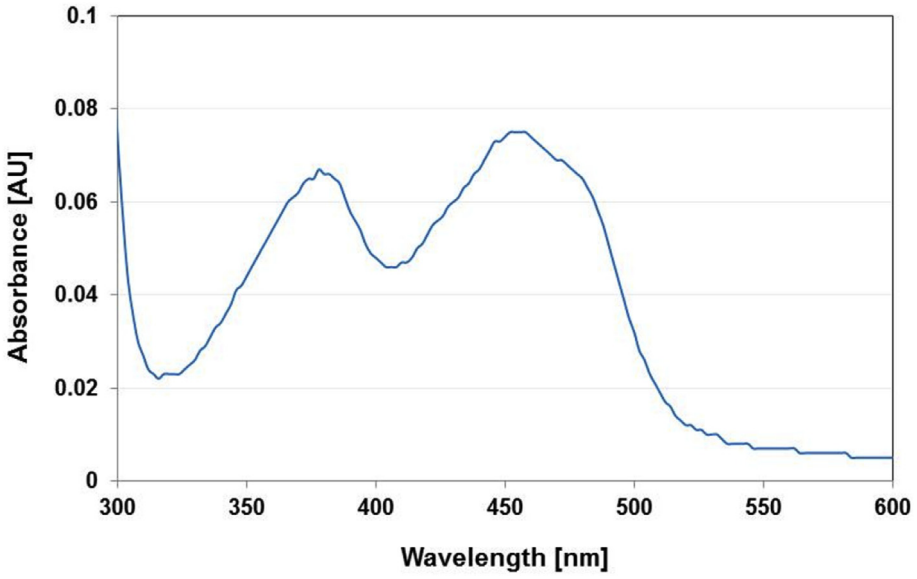

Fig. 2. UV/vis spectrum of 8.2 μM FgCPR in 150 mM phosphate buffer (pH 7.5) confirming the presence of fully oxidized flavins from the peaks in the region 300–500 nm.

desalted fractions evaporated overnight. The dry pellet was redissolved in 100 mM ABC and incubated with 1 μg trypsin or chymotrypsin (Pierce, ThermoFisherScientific, Hvidovre, Denmark) at 37 °C for 2 h. Nano-LC-MS/MS analysis and data treatment was done as described in Dionisio et al. [37].

2.4.3. Flavin incorporation and stoichiometry

Samples (100 μl of 265 μg/ml FgCPR) were denatured in 1 M citric acid (pH 1.6) and ultrafiltrated to 25 μl in a VivaSpin 500 ultrafiltration units (GE Healthcare, Brøndby, Denmark). The concentrate was washed with citric acid followed by MQ and the flow-through (FT) fractions were pooled. The protein concentrate was transferred with 2 × 250 μl MQ and quantified by Bradford (using BSA as a standard). FTs (containing FAD and FMN) were purified by SPE (Sep-pak Vac C18, Waters, Hedehusene, Denmark) and analyzed (50 μl) by HPLC-DAD (from Agilent Technologies, Glostrup, Denmark) on a Hypersil BDS C18 column, 250 × 2.1 mm i.d., 5 μm (Fischer Scientific, Roskilde, Denmark) at 30 °C using a linear gradient of 10–37% B over 12 min with eluents A) 5 mM ammonium acetate (pH 6.2) and B) MeOH and a flow rate of 0.25 ml/min. FAD and FMN were detected at 450 nm and quantified using external calibration curves. Results were corrected for flavin losses via recovery analysis calculated from mixed flavin spikes (800 ng/ml final) in 1 M citric acid, analyzed as described above. All samples were performed in triplicates and repeated once.

2.4.4. FgCPR kinetics

Reduction of MTT and cytochrome *c* (Cyt *c*) was performed in 96-well plates and analyzed using a BioTek Instruments Epoch microplate spectrophotometer (Holm & Halby, Brøndby, Denmark). Both assays were performed in 150 mM buffer (citrate for pH 5.5, PIPES for pH 6.5, phosphate for pH 7.5, tricine for pH 8.5 and sodium carbonate for pH 9.5) at 23 °C with an NADPH regeneration system (2.1 mM glucose-6-P (G-6-P), 0.7 mM $NADP^+$, 10 mM $MgCl_2$ and 0.7 U Glucose-6-*P*-Dehydrogenase (G6PDH), all obtained from Sigma-Aldrich, Brøndby, Denmark) which was charged for 30 min prior to initiation of the assay. For the MTT and Cyt *c* assays 20 nM FgCPR and 5 nM FgCPR were used, respectively. MTT or Cyt *c* substrate stock (10 times the final concentration) plus NADPH regeneration system in each buffer for the given pH were added to the wells and the plate was read prior to initiation of the assays to determine the initial absorbance ($A_{\lambda 0c}$) for each concentration of substrate. Assays were initiated by addition of FgCPR to a final volume of 250 μl. Samples were read every 10 s for 10 min at 610 nm and 550 nm for MTT and Cyt *c* reduction, respectively. The difference in absorbance was calculated according to $\Delta A = A_{\lambda tc} - A_{\lambda 0c}$ where $A_{\lambda tc}$ is the absorbance measured at time t for substrate concentration c. Concentrations of reduced MTT and reduced Cyt *c* were calculated from the extinction coefficients, $\varepsilon_{red.\ MTT} = 11.3\ mM^{-1}$ and $\varepsilon_{red.\ Cyt\ c} = 21.1\ mM^{-1}$ and a sample path length of 0.7 cm. Non-linear regression analysis was performed using GraphPad Prism software v. 7.02 (San Diego, CA, USA). All experiments were performed in triplicate and repeated at least twice.

3. Results

3.1. Purity, spectral analysis and aggregation state of FgCPR

NADPH-cytochrome P450 reductases from *Fusarium* sequence was selected from Uniprot.org (entry I1RZE7). This FgCPR sequence was chosen since it was the best characterized gene sequence and the only CPR sequence reviewed by experts for the Uniprot database. Submission of the full-length protein to TargetP server (http://www.cbs.dtu.dk/services/TargetP/) shows that the first 21 amino acids might belong to a leader peptide (LP) addressing the sequence to the secretion pathway. We removed this ER entry LP by PCR using the delta G-block synthetic gene construct as described in the Experimental section.

Forty milligrams of soluble N-terminally truncated (ΔN-t) protein was obtained from 16 g cells, which is considered a high expression level. Purity of the protein was assessed by SDS-PAGE analysis (see Fig. 1) with different amounts of protein loaded. Flavins were not incorporated into the apoform during expression in *E. coli* but were incorporated *in vitro* by incubation of the apoprotein with free flavins. UV/vis analysis (see Fig. 2) revealed associated flavins with the apo-proteins by spectra (in the region 300–500 nm) identical to that reported for other CPR flavoproteins [18,24].

Tryptic and chymotrypic digestion of the FgCPR proved that protein sequence matched the expected sequence expressed from

the *FgCPRΔ1-28* ORF (see Figure S 1 in Suppl. Mat.). The FgCPR eluted from the size exclusion column with a retention time of 26.5 min (see Fig. 3) corresponding to an apparent molecular weight of 89 kDa. The theoretical molecular weight of FgCPR is 77 kDa indicating that the protein exists in monomeric form.

3.2. Protein-flavin stoichiometry

Protein denaturation by heating or treatment with urea or guanidine did not released the bound flavins. Instead, citric acid (pH 1.6) was used for flavins release by temporary pH denaturation of the flavins binding pocket, and therefore, we could recover the protein quantitatively using VivaSpin ultrafiltration units. Recoveries of FAD and FMN, as assayed in the VivaSpin flow through, were determined to be 85% and 73%, respectively, by flavin quantifications using HPLC-DAD. Protein concentration by Bradford was determined to be 3.5 μM and FAD and FMN were quantified to 4.1 μM and 7.2 μM, respectively. This yields a final stoichiometry of 1:1:2 (FgCPR:FAD:FMN) in agreement with that reported for the yeast CPR by Lamb et al. [35].

3.3. FgCPR kinetics

Kinetics of the NADPH regeneration system for formation of NADPH from $NADP^+$ was virtually unaffected at pH 6.5–9.5. We also tested pH 5.5 for the regeneration system, however, no activity was observed for FgCPR at this pH for reduction of MTT or Cyt *c* with the NADPH regeneration system (or free NADPH) (data not shown).

3.3.1. Cytochrome c assay

The kinetic data for Cyt *c* reduction by FgCPR were fitted by non-linear regression analysis (see Fig. 4 and Table 1) using the regular Michaelis-Menten model of the GraphPad Prism software, from the equation:

$$V = \frac{V_{max} \cdot S}{K_m + S}$$

The assay was also tested at pH 6.5, however, no activity was observed below pH 7.5. Maximum binding (lowest K_m) and V_{max} was observed at pH 8.5. Since electrostatic interactions govern the binding between many cytochrome proteins to their reductase partners [38–41], the maximum rate and binding at pH 8.5 might be explained by an optimal electrostatic interaction. Increasing the pH further led to a decrease in both rate and binding of Cyt *c*.

Lamb et al. characterized full length and truncated yeast CPR using an NADPH regeneration system comparable to our studies except Lamb et al. did not include Mg^{2+} and they used 3 U of G6PDH [22] (we used 0.7 U G6PDH). The velocity was 9 times

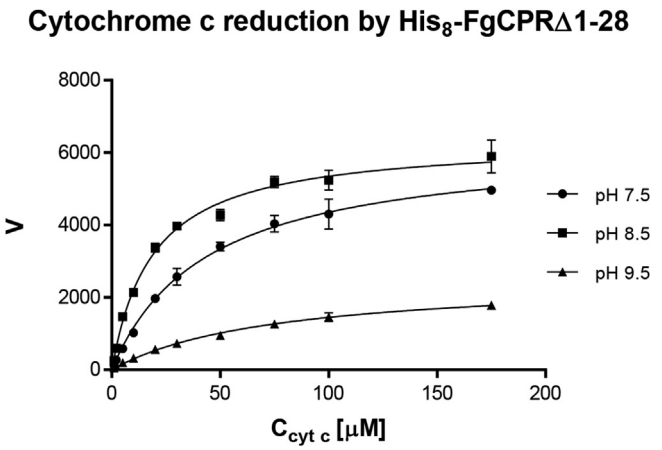

Fig. 4. Kinetic activity of FgCPR with cytochrome *c* as substrate at pH 7.5 (circles), 8.5 (squares) and 9.5 (triangles). V is given in nmoles/min/mg. Error bars are standard errors.

Table 1
Goodness of fit and kinetic parameters for FgCPR with cytochrome *c* as substrate.

	pH 7.5	pH 8.5	pH 9.5
R^2	0.976	0.975	0.972
V_{max}	6262 ± 274	6359 ± 184	2530 ± 160
K_m	43.9 ± 4.9	18.9 ± 1.9	74.6 ± 10

R^2 is goodness of fit for the kinetic data; V_{max} is given in nmoles/min/mg CPR; K_m is given in μM.

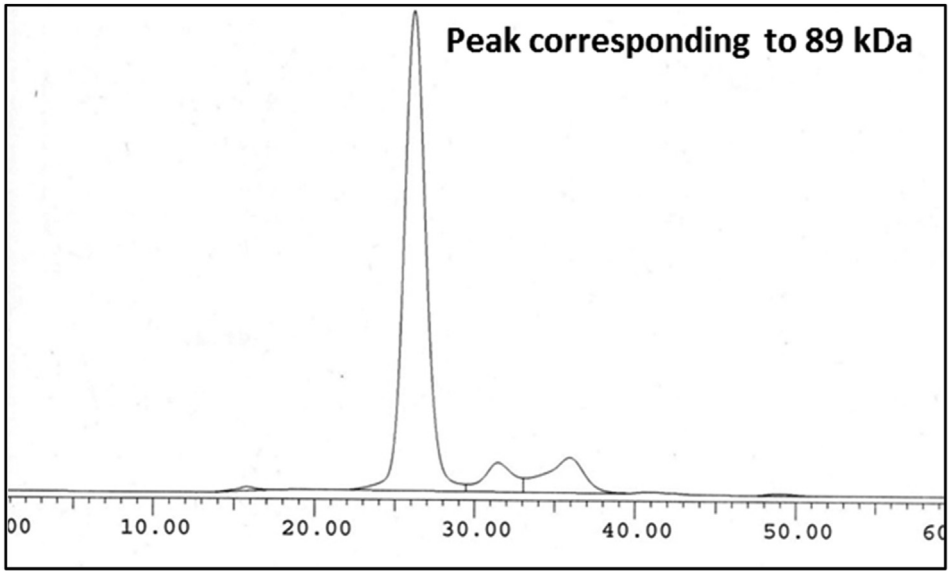

Fig. 3. Size exclusion chromatography of FgCPR obtained under conditions described in the experimental section. The apparent molecular weight (compared to protein markers) was 89 kDa suggesting the protein to be monomeric.

higher for their truncated *S. cerevisiae* CPR and the full-length reductase exhibited a V_{max} comparable to our FgCPR for the reduction of Cyt *c*. Cyt *c* interaction with the *S. cerevisiae* reductase at pH 7.5 was much stronger (K_m of 1–1.5 μM) than in our studies (K_m of 44 μM). Furthermore, two full-length NADPH-cytochrome P450 reductase proteins from *Capsicum annuum* exhibited kinetic parameters similar to our studies [42], with a K_m of 81 μM in 100 mM K-phosphate buffer (pH 7.6).

Microsomal cytochrome P450 reductase from *Liza saliens* liver had strong binding of Cyt *c* with a K_M of 7.69 μM and a rate 10 times (V_{max} of 47.6 μmol/min/mg) [43] compared to our FgCPR. Activity of the *L. saliens* CPR was also studied as a function of pH and found an optimum in the range pH 7.4–7.8 with a rapid decrease in activity outside this range using free NADPH (final concentration 162 μM) as electron donor.

In our studies, FgCPR reduction of Cyt *c* by free NADPH (initial concentration 400 μM) was most active for pH 7.5, while only minor or no activity could be observed at other tested pH values (data not shown). When employing the NADPH regeneration system, the optimum pH was 8.5 and the FgCPR still retained considerable activity at pH 9.5. Reduction of Cyt *c* using free NADPH was best described by an allosteric sigmoidal model (goodness of fit 0.94) and resulted in a much stronger association between FgCPR and Cyt *c* (K_m of 16 ± 2.5 μM). This suggests that components of the regeneration system can alter binding of Cyt *c* to the FgCPR compared to free NADPH. A reduction in V_{max} from 6262 ± 274 nmol/min/mg with the NADPH regeneration system to 5198 ± 224 nmol/min/mg when free NADPH was used, most likely due to a lack of NADPH regeneration.

4. MTT assay

Kinetic data for CPR with MTT as a substrate yielded the best fit using an allosteric sigmoidal model of the GraphPad Prism software based on the equation

$$V = \frac{V_{max} \cdot S^h}{EC_{50}{}^h + S^h}$$

where V is the CPR velocity, V_{max} is the maximum velocity for CPR (nmoles/min/mg), S is the substrate concentration (μM), h is the hill coefficient and EC_{50} is S resulting in 50% V_{max} (see Fig. 5 and Table 2).

The sigmoidal fit with corresponding hill coefficients of 1.6–1.9 shows that the reduction of MTT by CPR proceeds in a cooperative manner even at pH 6.5 which was the lowest pH value where our FgCPR exhibited kinetic activity.

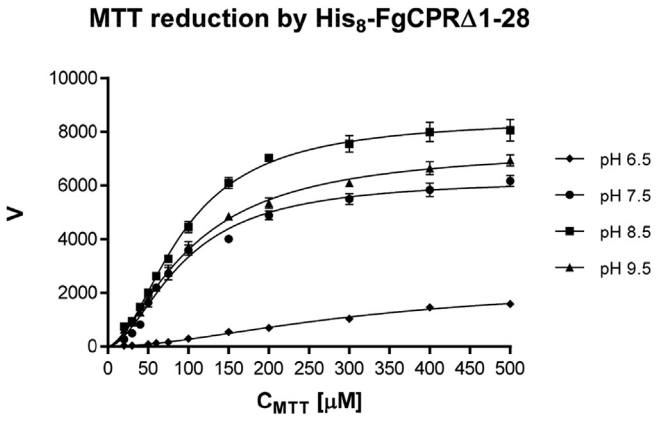

Fig. 5. Kinetic activity of FgCPR with MTT as substrate at pH 6.5 (diamonds), pH 7.5 (circles), 8.5 (squares) and 9.5 (triangles). V is given in nmoles/min/mg. Error bars are standard errors.

Table 2
Goodness of fit and kinetic parameters for FgCPR with MTT as substrate.

	pH 6.5	pH 7.5	pH 8.5	pH 9.5
R^2	0.979	0.977	0.987	0.989
V_{max}	2374 ± 336	6260 ± 208	8510 ± 204	7425 ± 212
EC_{50}	326 ± 59	92.8 ± 5.7	93.3 ± 4.1	104 ± 5.7
h	1.7 ± 0.2	1.8 ± 0.1	1.9 ± 0.1	1.6 ± 0.1

R^2 is goodness of fit for the kinetic data; V_{max} is given in nmoles/min/mg CPR; EC_{50} is given in μM, h is the hill coefficient.

Yim et al. [28] observed a kinetic activity 3–4 times higher for rat recombinant CPR compared to our FgCPR at pH 7.5 using an NADPH regeneration system with components in concentrations comparable to our study except Mg^{2+}. In our studies, K_m for MTT was higher than for Cyt *c*, but V_{max} for MTT was less affected by changes in pH. For pH 6.5 the velocity and binding to FgCPR for MTT was significantly decreased. This suggests that MTT binding is not governed primarily by electrostatic interactions as for Cyt *c*. V_{max} for MTT reduction, on the other hand, was affected by pH.

5. Discussion

5.1. FgCPR activity compared to other CPRs at pH 7.5

In general, we observed lower kinetic velocity (V_{max}) and weaker binding (higher K_m) compared to other truncated CPRs at pH 7.5. The reduced activity of our FgCPR compared to other truncated CPRs was initially suspected to stem from the N-terminal His_8-tag, which was uncleavable in spite of the presence of a TEV cleavage site (data not shown). However, for the *S. cerevisiae* CPR, the N-terminal region is located distinctly from all co-factor and cytochrome binding sites [44], and the presence of the His_8-tag should not directly interfere with NADPH or Cyt *c* binding. This is supported by studies of a tropinone reductase in which activity was strongly reduced when His-tagged at the C-terminus (the substrate binding site) but not with an N-terminal His-tag (opposite of the active site) [45]. Thus, the N-terminal His_8-tag should not influence activity of the FgCPR in our studies.

Since microsomal full-length reductase exhibits a V_{max} for Cyt *c* reduction comparable to that of our FgCPR, we speculate that the reduced rate of our FgCPR could be due to a non-optimal conformation of FgCPR. This would also explain the higher K_m (for Cyt *c*) for FgCPR compared to other CPRs. The comparison of a non-tagged to the FgCPR for activity and structure (*e.g.* X-ray) could reveal such information.

Another explanation might be that association with a membrane surface is more important for FgCPR for proper activity compared to other CPR proteins. Future studies with preparation of microsomal FgCPR could help clarify this.

5.2. Effect of substrate on kinetic activity

Interaction of CYP proteins and CPRs is governed by electrostatics. In addition, since membrane anchors are required for activity of some CPR-CYP pairs [21], restrictions for a proper co-alignment of such CPR-CYP pairs must apply. The small MTT only carries a single (permanent) positive charge, which explains why MTT binding to FgCPR is virtually unaffected by changes in pH. Furthermore, compared to Cyt *c*, fewer restrictions on alignment of MTT are required, which facilitates electron transfer and results in a higher V_{max}.

FgCPR reduction of Cyt *c* can be described using regular

Michaelis-Menten kinetics, whereas for the smaller MTT an allosteric sigmoidal model yielded the best fit. The reason for this is not entirely clear, since MTT reduction by other CPRs was described using a regular Michaelis-Menten model [28,46].

Our results from using Cyt *c* compared to MTT as substrates for FgCPR show that the reductase retains activity at alkaline pH but is sensitive to the type of substrate used.

5.3. Slightly alkaline pH yields optimal kinetics for the FgCPR

Theoretical pI values for Cyt *c* (equine heart) and FgCPR are 9.59 and 5.25, respectively, according to ExPASy [47]. At pH 9.5, Cyt *c* will be neutrally charged and FgCPR negatively charged. This will abolish most electrostatic interactions between FgCPR and Cyt *c*. However, since FgCPR activity was still observed at pH 9.5, the proteins must be able to interact with each other. Perhaps the relatively high ionic strength (150 mM carbonate) partially shields electrostatic repulsions at pH 9.5 still allowing binding between FgCPR and Cyt *c*.

It is possible that the pH optimum for the membrane bound full length FgCPR will be different than for the truncated FgCPR, since kinetics differ for full length and truncated versions of yeast CPR [22]. We also expressed and purified the full length FgCPR (data not shown), but were unable to incorporate flavins using the same approach as for the truncated FgCPR. Alternatively, full length CPR might be obtained from *F. graminearum* microsomes as for other CPRs [43,48,49]. Kinetic studies of the full length CPR from *F. graminearum* should be conducted with both detergent solubilization as well as reconstitution in liposomes mimicking the fungal membrane to evaluate the influence of the membrane system on protein activity. The sensitivity to substrate reduction illustrates that using only MTT or similar small molecule substrates might not be adequate for NADPH-cytochrome P450 reductase activity studies (where the natural substrate is a CYP), but might suffice for other types of reductases.

Intracellular pH changes with fungal changes and function, *e.g.* alkalinization of cytoplasm during cellular development of *C. albicans* [50] and during formation of macroconidia of *F. culmorum* [51]. In addition, the pH of the endoplasmic reticulum in HeLa cells is permeable to H^+ transfer to/from the cytosol [52]. Menke et al. showed that *F. graminearum* cellular morphology changes *in vitro* upon induction of trichothecene biosynthesis [53], *e.g.* with development of toxisomes harboring CYPs and a CPR involved in trichothecene biosynthesis [53].

Except for plants only one or two CPR genes have been putatively identified in eukaryotic species. The FgCPR characterized in this paper could therefore behave as a redox partner to one of the TRI proteins of the trichothecene pathway. This could also explain its optimal kinetic activity at pH 8.5 in agreement with studies by Menke et al. [53]. Alternatively, FgCPR might be a reductase partner involved in sterol or fatty acid biosynthesis in *F. graminearum*.

Acknowledgements

The Danish Council for Independent Research, Technology and Production Sciences is gratefully acknowledged for funding (project # 12-132600).

Appendix A. Supplementary data

Supplementary data related to this article can be found at http://dx.doi.org/10.1016/j.pep.2017.07.001.

References

[1] M. McMullen, R. Jones, D. Gallenberg, Scab of wheat and barley: a Re-emerging disease of devastating impact, Plant Dis. 81 (1997) 1340–1348. http://dx.doi.org/10.1094/PDIS.1997.81.12.1340.
[2] N.A. Foroud, F. Eudes, Trichothecenes in cereal grains, Int. J. Mol. Sci. 10 (2009) 147–173. http://dx.doi.org/10.3390/ijms10010147.
[3] C. Jansen, D. von Wettstein, W. Schäfer, K.-H. Kogel, A. Felk, F.J. Maier, Infection patterns in barley and wheat spikes inoculated with wild-type and trichodiene synthase gene disrupted *Fusarium graminearum*, Proc. Natl. Acad. Sci. U. S. A. 102 (2005) 16892–16897. http://dx.doi.org/10.1073/pnas.0508467102.
[4] R.H. Proctor, T.M. Hohn, S.P. McCormick, Reduced virulence of *Gibberella zeae* caused by disruption of a trichothecene toxin biosynthetic gene, Mol. Plant Microbe In. 8 (1995) 593–601. http://dx.doi.org/10.1094/mpmi-8-0593.
[5] M. Kimura, T. Tokai, N. Takahashi-Ando, S. Ohsato, M. Fujimura, Molecular and genetic studies of *Fusarium* trichothecene biosynthesis: pathways, genes, and evolution, Biosci. Biotechnol. Biochem. 71 (2007) 2105–2123. http://dx.doi.org/10.1271/bbb.70183.
[6] A.E. Desjardins, T.M. Hohn, S.P. McCormick, Trichothecene biosynthesis in *Fusarium* species: chemistry, genetics, and significance, Microbiol. Rev. 57 (1993) 595–604.
[7] A.E. Desjardins, R.D. Plattner, F. Vanmiddlesworth, Trichothecene biosynthesis in *Fusarium sporotrichioides*: origin of the oxygen atoms of T-2 toxin, Appl. Environ. Microb. 51 (1986) 493–497.
[8] S.P. McCormick, A.M. Stanley, N.A. Stover, N.J. Alexander, Trichothecenes: from simple to complex mycotoxins, Toxins 3 (2011) 802–814. http://dx.doi.org/10.3390/toxins3070802.
[9] T.M. Hohn, F. Vanmiddlesworth, Purification and characterization of the sesquiterpene cyclase trichodiene synthetase from *Fusarium sporotrichioides*, Archives Biochem. Biophys. 251 (1986) 756–761. http://dx.doi.org/10.1016/0003-9861(86)90386-3.
[10] T. Tokai, H. Koshino, N. Takahashi-Ando, M. Sato, M. Fujimura, M. Kimura, *Fusarium* Tri4 encodes a key multifunctional cytochrome P450 monooxygenase for four consecutive oxygenation steps in trichothecene biosynthesis, Biochem. Biophys. Res. Comm. 353 (2007) 412–417. http://dx.doi.org/10.1016/j.bbrc.2006.12.033.
[11] S.P. McCormick, N.J. Alexander, R.H. Proctor, *Fusarium* Tri4 encodes a multifunctional oxygenase required for trichothecene biosynthesis, Can. J. Microbiol. 52 (2006) 636–642. http://dx.doi.org/10.1139/w06-011.
[12] I.B. Meek, A.W. Peplow, C. Ake Jr., T.D. Phillips, M.N. Beremand, *Tri1* encodes the cytochrome P450 monooxygenase for C-8 hydroxylation during trichothecene biosynthesis in *Fusarium sporotrichioides* and resides upstream of another new *tri* gene, Appl. Environ. Microb. 69 (2003) 1607–1613. http://dx.doi.org/10.1128/aem.69.3.1607-1613.2003.
[13] N.J. Alexander, T.M. Hohn, S.P. McCormick, The *TRI11* gene of *Fusarium sporotrichioides* encodes a cytochrome P-450 monooxygenase required for C-15 hydroxylation in trichothecene biosynthesis, Appl. Environ. Microb. 64 (1998) 221–225.
[14] T. Lee, Y.-K. Han, K.-H. Kim, S.-H. Yun, Y.-W. Lee, *Tri13* and *Tri7* determine deoxynivalenol- and nivalenol-producing chemotypes of gibberella zeae, Appl. Environ. Microb. 68 (2002) 2148–2154. http://dx.doi.org/10.1128/AEM.68.5.2148-2154.2002.
[15] X. Liu, F. Yu, G. Schnabel, J. Wu, Z. Wang, Z. Ma, Paralogous *cyp51* genes in *Fusarium graminearum* mediate differential sensitivity to sterol demethylation inhibitors, Fungal Genet. Biol. 48 (2011) 113–123. http://dx.doi.org/10.1016/j.fgb.2010.10.004.
[16] L.J. Harris, N.J. Alexander, A. Saparno, B. Blackwell, S.P. McCormick, A.E. Desjardins, L.S. Robert, N. Tinker, J. Hattori, C. Piche, J.P. Schernthaner, R. Watson, T. Ouellet, A novel gene cluster in *Fusarium graminearum* contains a gene that contributes to butenolide synthesis, Fungal Genet. Biol. 44 (2007) 293–306. http://dx.doi.org/10.1016/j.fgb.2006.11.001.
[17] A. Bahadoor, D. Schneiderman, L. Gemmill, W. Bosnich, B. Blackwell, J.E. Melanson, G. McRae, L.J. Harris, Hydroxylation of longiborneol by a *clm2*-encoded CYP450 monooxygenase to produce culmorin in Fusarium graminearum, J. Nat. Prod. 79 (2016) 81–88. http://dx.doi.org/10.1021/acs.jnatprod.5b00676.
[18] Cytochrome P450: Structure, Mechanism and Biochemistry, Kluwer Academic/plenum Publishers, 233 Spring Street, New York, NY, US, 2004.
[19] P.A. Hubbard, A.L. Shen, R. Paschke, C.B. Kasper, J.-J.P. Kim, NADPH-cytochrome P450 oxidoreductase: structural basis for hydride and electron transfer, J. Biol. Chem. 276 (2001) 29163–29170. http://dx.doi.org/10.1074/jbc.M101731200.
[20] L. Lah, N. Kraševec, P. Trontelj, R. Komel, High diversity and complex evolution of fungal cytochrome P450 reductase: cytochrome P450 systems, Fungal. Genet. Biol. 45 (2008) 446–458. http://doi.org/10.1016/j.fgb.2007.10.004.
[21] S.D. Black, J.S. French, C.H. Williams Jr., M.J. Coon, Role of a hydrophobic polypeptide in the N-terminal region of NADPH-cytochrome P-450 reductase in complex formation with P-450lm, Biochem. Biophys. Res. Comm. 91 (1979) 1528–1535. http://dx.doi.org/10.1016/0006-291X(79)91238-5.
[22] D.C. Lamb, A.G. Warrilow, K. Venkateswarlu, D.E. Kelly, S.L. Kelly, Activities and kinetic mechanisms of native and soluble NADPH-cytochrome P450 reductase, Biochem. Biophys. Res. Comm. 286 (2001) 48–54. http://dx.doi.org/10.1006/bbrc.2001.5338.

[23] T. Makovec, K. Breskvar, Catalytic and immunochemical properties of NADPH-cytochrome P450 reductase from fungus Rhizopus nigricans, J. Steroid. Biochem. 82 (2002) 89–96. http://dx.doi.org/10.1016/S0960-0760(02)00145–0.
[24] K. Venkateswarlu, D.C. Lamb, D.E. Kelly, N.J. Manning, S.L. Kelly, The N-terminal membrane domain of yeast NADPH-cytochrome P450 (CYP) oxidoreductase is not required for catalytic activity in sterol biosynthesis or in reconstitution of CYP activity, J. Biol. Chem. 273 (1998) 4492–4496.
[25] A.L. Shen, T.D. Porter, T.E. Wilson, C.B. Kasper, Structural analysis of the FMN binding domain of NADPH-cytochrome P-450 oxidoreductase by site-directed mutagenesis, J. Biol. Chem. 264 (1989) 7584–7589.
[26] F.P. Guengerich, M.V. Martin, C.D. Sohl, Q. Cheng, Measurement of cytochrome P450 and NADPH-cytochrome P450 reductase, Nat. Protoc. 4 (2009) 1245–1251. http://dx.doi.org/10.1038/nprot.2009.121.
[27] S.K. Yim, S.J. Yun, C.H. Yun, A continuous spectrophotometric assay for NADPH-cytochrome P450 reductase activity using 1,1-diphenyl-2-picrylhydrazyl, J. Biochem. Mol. Biol. 37 (2004) 629–633. http://dx.doi.org/10.5483/BMBRep.2004.37.5.629.
[28] S.K. Yim, C.H. Yun, T. Ahn, H.C. Jung, J.G. Pan, A continuous spectrophotometric assay for NADPH-cytochrome P450 reductase activity using 3-(4,5-dimethylthiazol-2-yl)-2,5-diphenyltetrazolium bromide, J. Biochem. Mol. Biol. 38 (2005) 366–369.
[29] T. Fujii, N. Takaya, Denitrification by the fungus *Fusarium oxysporum* involves NADH-nitrate reductase, Biosci. Biotechnol. Biochem. 72 (2008) 412–420. http://dx.doi.org/10.1271/bbb.70538.
[30] A.V. Kurakov, A.N. Nosikov, E.V. Skrynnikova, N.P. L'vov, Nitrate reductase and nitrous oxide production by *Fusarium oxysporum* 11dn1 under aerobic and anaerobic conditions, Curr. Microbiol. 41 (2000) 114–119. http://dx.doi.org/10.1007/s002840010104.
[31] E.V. Morozkina, A.V. Kurakov, A.N. Nosikov, E.V. Sapova, N.P. L'vov, Properties of nitrate reductase from *Fusarium oxysporum* 11dn1 fungi grown under anaerobic conditions, Appl. Biochem. Microbiol. 41 (2005) 254–258. http://dx.doi.org/10.1007/s10438-005-0043-3.
[32] C.A. Cuomo, U. Guldener, J.R. Xu, F. Trail, B.G. Turgeon, A. Di Pietro, J.D. Walton, L.J. Ma, S.E. Baker, M. Rep, G. Adam, J. Antoniw, T. Baldwin, S. Calvo, Y.L. Chang, D. Decaprio, L.R. Gale, S. Gnerre, R.S. Goswami, K. Hammond-Kosack, L.J. Harris, K. Hilburn, J.C. Kennell, S. Kroken, J.K. Magnuson, G. Mannhaupt, E. Mauceli, H.W. Mewes, R. Mitterbauer, G. Muehlbauer, M. Munsterkotter, D. Nelson, K. O'Donnell, T. Ouellet, W. Qi, H. Quesneville, M.I. Roncero, K.Y. Seong, I.V. Tetko, M. Urban, C. Waalwijk, T.J. Ward, J. Yao, B.W. Birren, H.C. Kistler, The *Fusarium graminearum* genome reveals a link between localized polymorphism and pathogen specialization, Science (New York, N.Y.) 317 (2007) 1400–1402. http://dx.doi.org/10.1126/science.1143708.
[33] G.J. Chen, N. Qiu, C. Karrer, P. Caspers, M.G.P. Page, Restriction site-free insertion of PCR products directionally into vectors, Biotechniques 28 (2000) 498–505.
[34] F. van den Ent, J. Lowe, RF cloning: a restriction-free method for inserting target genes into plasmids, J. Biochem. Bioph. Meth. 67 (2006) 67–74. http://dx.doi.org/10.1016/j.jbbm.2005.12.008.
[35] D.C. Lamb, Y. Kim, L.V. Yermalitskaya, V.N. Yermalitsky, G.I. Lepesheva, S.L. Kelly, M.R. Waterman, L.M. Podust, A second FMN binding site in yeast NADPH-cytochrome P450 reductase suggests a mechanism of electron transfer by diflavin reductases, Structure (Lond. Engl 1993) 14 (2006) 51–61. http://dx.doi.org/10.1016/j.str.2005.09.015.
[36] D.D. Oprian, M.J. Coon, Oxidation-reduction states of FMN and FAD in NADPH-cytochrome P-450 reductase during reduction by NADPH, J. Biol. Chem. 257 (1982) 8935–8944.
[37] G. Dionisio, C.K. Madsen, P.B. Holm, K.G. Welinder, M. Jorgensen, E. Stoger, E. Arcalis, H. Brinch-Pedersen, Cloning and characterization of purple acid phosphatase phytases from wheat, barley, maize, and rice, Plant Physiol. 156 (2011) 1087–1100. http://dx.doi.org/10.1104/pp.110.164756.
[38] A. Bridges, L. Gruenke, Y.T. Chang, I.A. Vakser, G. Loew, L. Waskell, Identification of the binding site on cytochrome P450 2B4 for cytochrome b5 and cytochrome P450 reductase, J. Biol. Chem. 273 (1998) 17036–17049.
[39] S. Shen, H.W. Strobel, Role of lysine and arginine residues of cytochrome P450 in the interaction between cytochrome P4502B1 and NADPH-cytochrome P450 reductase, Arch. Biochem. Biophys. 304 (1993) 257–265.
[40] S.J. Shen, H.W. Strobel, Probing the putative cytochrome P450- and cytochrome *c*-binding sites on NADPH-cytochrome P450 reductase by anti-peptide antibodies, Biochemistry 33 (1994) 8807–8812. http://dx.doi.org/10.1021/bi00195a024.
[41] T. Shimizu, T. Tateishi, M. Hatano, Y. Fujii-Kuriyama, Probing the role of lysines and arginines in the catalytic function of cytochrome P450d by site-directed mutagenesis. Interaction with NADPH-cytochrome P450 reductase, J. Biol. Chem. 266 (1991) 3372–3375.
[42] G.-Y. Lee, H.M. Kim, S.H. Ma, S.H. Park, Y.H. Joung, C.-H. Yun, Heterologous expression and functional characterization of the NADPH-cytochrome P450 reductase from Capsicum annuum, Plant Physiol. Biochem. 82 (2014) 116–122. http://dx.doi.org/10.1016/j.plaphy.2014.05.010.
[43] A. Sen, E. Arinc, Purification and characterization of cytochrome P450 reductase from liver microsomes of feral leaping mullet (*Liza saliens*), J. Biochem. Mol. Toxicol. 12 (1998) 103–113.
[44] M. Wang, D.L. Roberts, R. Paschke, T.M. Shea, B.S. Masters, J.J. Kim, Three-dimensional structure of NADPH-cytochrome P450 reductase: prototype for FMN- and FAD-containing enzymes, P. Natl. A. Sci. U. S. A. 94 (1997) 8411–8416.
[45] A.C. Freydank, W. Brandt, B. Drager, Protein structure modeling indicates hexahistidine-tag interference with enzyme activity, Proteins 72 (2008) 173–183. http://dx.doi.org/10.1002/prot.21905.
[46] S.-H. Park, J.-Y. Kang, D.-H. Kim, T. Ahn, C.-H. Yun, The flavin-containing reductase domain of cytochrome P450 BM3 acts as a surrogate for mammalian NADPH-P450 reductase, Biomol. Ther. 20 (2012) 562–568. http://dx.doi.org/10.4062/biomolther.2012.20.6.562.
[47] E. Gasteiger, A. Gattiker, C. Hoogland, I. Ivanyi, R.D. Appel, A. Bairoch, ExPASy: the proteomics server for in-depth protein knowledge and analysis, Nucleic Acids Res. 31 (2003) 3784–3788.
[48] T. Makovec, K. Breskvar, Purification and characterization of NADPH-cytochrome P450 reductase from filamentous fungus Rhizopus nigricans, Arch. Biochem. Biophys. 357 (1998) 310–316. http://dx.doi.org/10.1006/abbi.1998.0824.
[49] J.G.T. Menting, E. Cornish, R.K. Scopes, Purification and partial characterization of NADPH-cytochrome *c* reductase from *Petunia hybrida* flowers, Plant Physiol. 106 (1994) 643–650. http://dx.doi.org/10.1104/pp.106.2.643.
[50] E. Stewart, N.A. Gow, D.V. Bowen, Cytoplasmic alkalinization during germ tube formation in Candida albicans, J. Gen. Microbiol. 134 (1988) 1079–1087. http://dx.doi.org/10.1099/00221287-134-5-1079.
[51] G.S. Chitarra, P. Breeuwer, F.M. Rombouts, T. Abee, J. Dijksterhuis, Differentiation inside multicelled macroconidia of *Fusarium culmorum* during early germination, Fungal. Genet. Biol. 42 (2005) 694–703. http://dx.doi.org/10.1016/j.fgb.2005.04.001.
[52] J.H. Kim, L. Johannes, B. Goud, C. Antony, C.A. Lingwood, R. Daneman, S. Grinstein, Noninvasive measurement of the pH of the endoplasmic reticulum at rest and during calcium release, Proc. Natl. Acad. Sci. U. S. A. 95 (1998) 2997–3002.
[53] J. Menke, J. Weber, K. Broz, H.C. Kistler, Cellular development associated with induced mycotoxin synthesis in the filamentous fungus Fusarium graminearum, PLoS One 8 (2013) e63077. http://dx.doi.org/10.1371/journal.pone.0063077.